

## Lévy-taxis: a novel search strategy for finding odor plumes in turbulent flow-dominated environments

This article has been downloaded from IOPscience. Please scroll down to see the full text article.

2009 J. Phys. A: Math. Theor. 42 434010

(<http://iopscience.iop.org/1751-8121/42/43/434010>)

View [the table of contents for this issue](#), or go to the [journal homepage](#) for more

Download details:

IP Address: 171.66.16.155

The article was downloaded on 03/06/2010 at 08:14

Please note that [terms and conditions apply](#).

# Lévy-taxis: a novel search strategy for finding odor plumes in turbulent flow-dominated environments

Zohar Pasternak<sup>1,4</sup>, Frederic Bartumeus<sup>2,3</sup> and Frank W Grasso<sup>1</sup>

<sup>1</sup> BioMimetic and Cognitive Robotics Laboratory, Department of Psychology, Brooklyn College, The City University of New York, 2900 Bedford Avenue, Brooklyn 11210, NY, USA

<sup>2</sup> Department of Ecology and Evolutionary Biology & Princeton Environmental Institute, 106 Guyot Hall, Princeton University, Princeton 08544, NJ, USA

<sup>3</sup> Institut Català de Ciències del Clima, Baldiri i Reixach 2, 08028 Barcelona, Catalonia, Spain

E-mail: [zpast@yahoo.com](mailto:zpast@yahoo.com)

Received 5 January 2009, in final form 30 March 2009

Published 13 October 2009

Online at [stacks.iop.org/JPhysA/42/434010](http://stacks.iop.org/JPhysA/42/434010)


## Abstract

Locating chemical plumes in aquatic or terrestrial environments is important for many economic, conservation, security and health related human activities. The localization process is composed mainly of two phases: finding the chemical plume and then tracking it to its source. Plume tracking has been the subject of considerable study whereas plume finding has received little attention. We address here the latter issue, where the searching agent must find the plume in a region often many times larger than the plume and devoid of the relevant chemical cues. The probability of detecting the plume not only depends on the movements of the searching agent but also on the fluid mechanical regime, shaping plume intermittency in space and time; this is a basic, general problem when exploring for ephemeral resources (e.g. moving and/or concealing targets). Here we present a bio-inspired search strategy named Lévy-taxis that, under certain conditions, located odor plumes significantly faster and with a better success rate than other search strategies such as Lévy walks (LW), correlated random walks (CRW) and systematic zig-zag. These results are based on computer simulations which contain, for the first time ever, digitalized real-world water flow and chemical plume instead of their theoretical model approximations. Combining elements of LW and CRW, Lévy-taxis is particularly efficient for searching in flow-dominated environments: it adaptively controls the stochastic search pattern using environmental information (i.e. flow) that is available throughout the course of the search and shows correlation with the source providing the cues. This strategy finds natural application in real-world search missions, both by humans and autonomous robots, since it accommodates the stochastic nature of chemical mixing in turbulent flows. In addition, it may prove useful in the

<sup>4</sup> Author to whom any correspondence should be addressed.

field of behavioral ecology, explaining and predicting the movement patterns of various animals searching for food or mates.

PACS number: 05.40.Fb

 This article has associated online supplementary data files

## Introduction

The study of search strategies has, in the past 20 years, witnessed immense growth in scientific attention. Research has concentrated on two areas: biological encounter rates and the plume-tracking problem. The field of biological encounters deals with strategies of various animals for searching randomly located targets (food, mates, etc) whose exact locations are not known *a priori* [1], whereas plume-tracking deals with strategies (either biological, biomimetic or bio-inspired) for traveling upstream inside an odor plume created by a target, thus reaching the source of the odor (i.e. the target) [2]. Concordantly, when attempting to locate the source of a chemical plume in aquatic or terrestrial environments, the localization process is composed mainly of these two phases: first, finding the chemical plume in a large, odorless environment ('plume finding') and second, tracking the plume to its source ('plume tracking'). Numerous navigation strategies have been developed with the aim of enabling robots or simulated agents to perform plume tracking, i.e. to perform a local search inside a plume and find its source based on the spatial distribution of the chemical cue emanating from the source [3–9]. All these strategies assume that the robot starts its search with knowledge of the plume location or simply start their search within or very near the plume. Efforts to solve this problem, however, have rarely acknowledged the practical reality that before plume-tracking strategies can be employed, the plume itself must be located, and to date, no published study has quantitatively tackled this task of plume finding in a large area devoid of the relevant chemical cue(s). Plume finding is important inasmuch the intermittent behavior of the plume can generate vast cueless regions at similar spatio-temporal scales as those of the search process itself.

An efficient search process depends on maximizing the chances for detecting the target while minimizing the time and resources consumed en-route. In real world applications spanning more than several hundred meters, efficient area coverage to find ephemeral chemical cues that are sparsely distributed in space is a formidable problem. First, detecting the plume does not involve merely a simple spatial search but is rather a function both of space and time—plume-detection probability depends on when a given point in space is sampled. In other words, the intermittency of chemical signals produced by turbulent flow means that a robot that enters the 'plume region' is not guaranteed to detect the chemical [10, 11]. This is a basic, general problem when exploring for ephemeral resources (e.g. moving and/or concealing targets). Second, time constraints: searching agents have a limited amount of time to perform their mission. For example, energy supply of searchers may be limited, targets may remain in place for a limited amount of time or the mission itself may be urgent [12]. Therefore, a good large-scale plume-finding search strategy must be able to return to previously searched areas (to account for plume intermittency) yet still cover a lot of space in a limited amount of time. Since chemical plumes are patchy in space and intermittent in time, large-scale plume finding poses a stochastic search problem, and its solutions may generalize to other domains of stochastic search efforts that involve intermittent cues.

In 'Lévy-taxis', the search strategy we introduce here, the searching agent uses local information from the ambient flow as a surrogate cue for the absent chemical one in

combination with a large-scale stochastic search strategy. The approach exploits the mass transfer principles of fluid mechanics that require the spatial trajectories of chemicals carried by a turbulent flow to be spatially and temporally correlated with the flow itself, on its path from the chemical source. Importantly, the local flow cue provides environmental adaptability to the large-scale stochastic search strategy [13]. To evaluate its efficiency and applicability, the Lévy-taxis search strategy was tested in a simulator with dynamic chemical dispersal and flow kinematics. A two-dimensional real-world flow and a chemical plume from a digitalized database [10] were supplied to the agents to guide their decision making (see Materials and methods). We compared the performance of Lévy-taxis to that of a Brownian walk (BW), Lévy walks [14] (LW), correlated random walks [15] (CRW) and a deterministic zig-zag strategy (ZZ) under the simulated conditions. By ‘playing-back’ recorded odor plume distribution and water flow data we were able to test the search strategies using real fluid mechanics with appropriate correlations between flow and chemical cues; in addition, it allowed us to compare the five search strategies under identical and reproducible environmental conditions, a feat that would be impossible in a real physical robotic implementation because of the chaotic nature of real-world conditions. We quantified performance in terms of the probability of detecting the plume as a percentage of detection success (DS) over a fixed number of trials, and a net-to-gross displacement ratio (NGDR) defined as the percentage ratio of the shortest linear distance between the start and the plume detection point and the total travel distance. The agents used in our simulations traveled with a constant speed so the NGDR was directly related to the time spent in the exploration process; the higher the NGDR, the more direct the path taken to the plume.

## Materials and methods

### Overview

Lévy-taxis, along with the four other area-coverage search strategies, were tested under identical conditions: (1) Brownian walk, in which the move lengths (ML) are taken from an asymptotically Gaussian-like distribution ( $\mu = 3$ ) and the turning angles (TA) are sampled from a uniform distribution ( $\rho = 0$ ); (2) Lévy walks [14], in which TA are uniformly distributed ( $\rho = 0$ ) but ML follow a power-law distribution with Lévy index  $\mu$  ( $1 < \mu \leq 3$ ), representing the tail of a Lévy-stable distribution; (3) correlated random walks [15], in which ML are taken from an asymptotically Gaussian-like distribution ( $\mu = 3$ ) and TA follows a wrapped Cauchy distribution centered on the ‘upstream’ angle ( $0 \leq \rho \leq 1$ ); (4) Lévy-taxis, in which TA follows a wrapped Cauchy distribution centered on the ‘upstream’ angle ( $0 \leq \rho \leq 1$ ) while ML follows a power-law (Lévy) distribution ( $1 < \mu \leq 3$ ); and (5) a deterministic zig-zag, where TA remain constant throughout the run and ML reach from one cross-stream boundary to the other. Under each combination of parameters  $\mu$  and  $\rho$  (for the four stochastic strategies) and TA (for zig-zag) the simulation was repeated for  $N = 50$  runs, each run ending in failure ( $P = 0$ ) if the upstream boundary was reached without detecting the plume or success ( $P = 1$ ) if the plume was detected. If the searcher reached any of the two cross-stream boundaries, its step was truncated and a new step began immediately. Since background levels of the chemical signal (i.e. noise) reached as high as 0.28% of its concentration at the source, the agent’s chemical detection threshold was set to 0.30%. A detection success index (DS) was calculated as the percentage of trials in which the plume was detected,  $DS = \frac{N_{P=1}}{N} \times 100$ . For runs that managed to detect the plume, we calculated the net-to-gross displacement ratio as  $NGDR = (ND/TD) \times 100$ , where ND is the net displacement, i.e. the shortest distance between the trajectory start and end points, and TD is the total traveled distance. The endpoint

was chosen to be the point where the plume was detected (i.e. sensed chemical level reached or surpassed 0.3% of its level at the source); therefore the NGDR measurement was interpreted as an index of the path directedness to the target, directly measuring the amount of time spent until reaching the search goal, going from 100 (minimum time expenditure) to 0 (maximum time expenditure). Between  $1.0 \leq \mu \leq 2.6$ ,  $\mu$  was tested in increments of 0.2, with  $N = 50$  at each tested value; however, it was hypothesized that detection success would peak between  $2.6 \leq \mu \leq 3.0$ , so in this region  $\mu$  was tested in increments of 0.1 (to achieve a finer resolution), and  $N = 50$  was repeated 5 times (to achieve a standard deviation value for the ‘detection success’ index). Similarly, between  $0.2 \leq \rho \leq 1.0$ ,  $\rho$  was tested in increments of 0.1, with  $N = 50$  at each tested value; however, it was hypothesized that detection success would peak between  $0.0 \leq \rho \leq 0.2$ , so in this region  $\rho$  was tested in increments of 0.05 (to achieve a finer resolution), and  $N = 50$  was repeated 5 times (to achieve a standard deviation value for the ‘detection success’ index).

### *The computerized simulation environment*

We created a virtual agent navigating a bounded, flow-dominated river-like computerized environment. The river-like environment can be considered either as a literal model for a river or as a search-region boundary; any real-world application faces such a limitation either because of real physical boundaries or energy limitations for the searching agent. The simulator software itself was originally developed by Professor Jay Farrell (University of California, Riverside), and we subsequently enhanced it with a digital ‘playback’ of an actual, real-world flow field and chemical plume obtained using a coupled PIV-LIF (particle image velocimetry–laser-induced fluorescence) technique [10]. The dye plume and flow field in a laboratory flow-tank were digitally captured in a 19 Hz, 150 s database; this specific scalar plume, constantly emanating from a point source in a turbulent boundary layer, was exhaustively studied and described in [10] (see also supplementary video of the plume. [stacks.iop.org/JPhysA/42/434010](http://stacks.iop.org/JPhysA/42/434010). The video is sped up  $\times 6$  times in order to enable the reader to better comprehend its structure and meander). To our knowledge, this is the first published record of an underwater robotic simulation environment being integrated with a real-world scalar plume in a turbulent boundary layer flow. As this database only spanned  $52 \times 52$  cm, we scaled it up using Cowen *et al*’s simple zeroth-order approach (personal communication): by ignoring viscosity, an assumption that still preserves the physics of the large-scale turbulent eddies, i.e. the concentration and velocity fields, we get a simple scaling  $(C/C_0)_P = (C/C_0)_M$ , where  $C$  is the local chemical concentration,  $C_0$  is the source concentration, and  $P$  and  $M$  refer to prototype (desired scale) and model (actual data), respectively. This equation states that for geometrically similar situations with iso-kinetic releases, the non-dimensional concentration remains unchanged. Now, if  $L$  and  $U$  are the length and velocity scale respectively, then the ratios  $L_P/L_M$  and  $U_P/U_M$  are decoupled and can be arbitrarily chosen; time between concentration measurements ( $t$ ) is scaled by  $t_P/t_M = (L_P/L_M) \times (U_M/U_P)$  and the length scale of the sample area (i.e. pixel size,  $\nabla$ ) is given by  $\nabla_P/\nabla_M = L_P/L_M$ . In our study, the flow field data set was ‘tiled’ (i.e. copied)  $\times 4$  in the  $x$ -axis (downstream) to form a  $0.52 \times 2.08$  m model, which was then up-scaled by a factor of 192.3 to create a  $100 \times 400$  m river-like prototype (simulation environment, figure 1). The chemical plume data set was ‘tiled’  $\times 3$  in the  $x$ -axis (downstream) to form a  $0.52 \times 1.56$  m chemical plume model, which was then up-scaled by a factor of 38.5 to create a  $20 \times 60$  m prototype (figure 1). As the model plume data set characteristics were  $L_M = 0.52$  m,  $U_M = 0.08$  m s<sup>-1</sup>,  $\nabla_M = 0.5$  mm and  $t_M = 0.052$  s (19 Hz), the eventual ‘river’ prototype (with a scaled-up flow speed of  $U_P = 1$  ms<sup>-1</sup>) resulted in  $t_P = 0.16$  s and  $\nabla_P = 96$  mm. In other words, the agent’s chemical sampling rate in the scaled-up

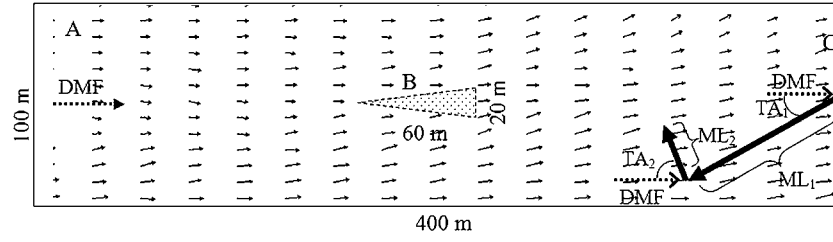


**Figure 1.** Schematic of the simulation environment and search strategies (move lengths and simulation environment not to scale). (A) Turbulent boundary layer flow; angle of small arrows indicates local flow angle while arrow length indicates flow speed. (B) Odor plume, flowing downstream. Time-averaging the chemical concentration values of the plume creates a triangular shape. DMF (dotted arrows), direction of mean flow. (C) Agent trajectory, starting at the middle of the downstream boundary and ending when it first discovers the plume (‘success’) or reaches the upstream boundary (‘failure’). Thick arrows, continuous ‘flights’ taken by the agent (two flights are shown);  $TA_x$ , turning angle ( $x$  denotes the sequential number of the flight);  $ML_x$ , move length.

prototype was a realistic 6.3 Hz, and its spatial sampling resolution was just below 10 cm—a very realistic resolution for an underwater chemical sensor. The agent ground speed was set to  $1.5 \text{ m s}^{-1}$  (a typical speed for small AUVs), its memory size (time for averaging flow direction measurements) to 3 s, and its minimal step length (representing minimal turning radius) to 5 m. The maximum level of background chemical noise in our real-life chemical plume data set was found to be  $C/C_0 = 0.0028$  (i.e. 0.28% of the maximal, source concentration), so in order to minimize false detections, the threshold for the agent’s chemical sensor was set to  $C/C_0 = 0.003$  (0.3% of source concentration).

#### The Lévy-taxis strategy

The move lengths ( $l$ ) of Lévy-taxis are taken from a power-law distribution as in a Lévy walk (i.e.  $P(l) \sim l^{-\mu}$ ,  $1 < \mu \leq 3$ ), and the turning angles ( $\theta$ ) are drawn from a wrapped Cauchy distribution as in a CRW process

$$\left( P(\theta) \sim \frac{1 - \rho^2}{2\pi(1 + \rho^2 - 2\rho \cos(\theta))}, \quad \rho \in [0, 1] \right).$$

The move lengths are not instantaneous but instead are ‘walked’ with constant velocity, i.e.  $v = 1.5 \text{ m s}^{-1}$ , being the underlying model a Lévy walk and not a Lévy flight [14]. The corresponding sampling functions are obtained directly applying the inversion method on the probability distributions. For the move lengths we obtain:  $l = l_0 \times r^{\frac{1}{1-\mu}}$ , where  $\mu$  is the Lévy index ( $1 < \mu \leq 3$ ),  $l_0$  is the minimum move length, and  $r$  is a uniformly distributed random variable  $r \in [0, 1]$ . As  $\mu$  increases, the probability of long steps diminishes and with it the directional persistence; conversely, as  $\mu$  diminishes, the probability of long move lengths increases and so does the directional persistence. As the concepts of ‘short’ and ‘long’ step lengths depend greatly upon the physical scale of the agent,  $l_0$  adjusts the move lengths to a scale characteristic of the specific agent, representing the agent’s size, inertia and minimal turning radius (in our experiments,  $l_0 = 5 \text{ m}$ ). For the turning angles, the sampling function reads

$$\theta = \left[ 2 \times \arctan \left( \frac{(1 - \rho) \times \tan(\pi \times (r - 0.5))}{1 + \rho} \right) \right] + \text{DMF} + 180^\circ,$$

where  $\rho$  is the shape parameter ( $0 \leq \rho \leq 1$ ), DMF stands for the direction of the mean flow in degrees and  $r$  is a uniformly distributed random variable  $r \in [0, 1]$ . This is so because in a

standard CRW the turning angle distribution is centered at zero (so that the most likely action at each step is to keep forward at the same direction as in the previous step). In Lévy-taxis, however, motion is environmentally adaptive, meaning that the turning angle distribution is centered at the local upstream flow direction so that the most likely action at each step is to go upstream. The stochastic sampling of the deviations (distributed as a wrapped Cauchy) from the upstream flow angle is performed at the beginning of each walk, so that within each walk this deviation remains fixed. In such a way, one can intermittently control the angular or directional correlations in the walk according to the main direction of the flow, creating a Lévy walk in a flow-centered frame of reference. Qualitatively, the Lévy-taxis strategy combines recently suggested large-scale stochastic search models [13]—the Lévy walks [14, 16, 17] (LW) and the correlated random walks [15, 18, 19] (CRW)—with the incorporation of motion adaptiveness based on local environmental information such as flow or odor plumes [20, 21] to create new search behaviors.

### *The other search strategies*

Aside from the Lévy-taxis strategy, four search strategies were tested under the same simulated conditions (figure 1). First, zig-zag, where the agent trajectory starts at the middle of the downstream boundary, moves in a turning angle (TA) according to the DMF (direction of mean flow), and continues in a zig-zag motion whenever it reaches either of the cross-stream boundaries, TA remaining constant during the whole search. In order to fully test the zig-zag strategy, each one of the  $N = 50$  runs was started 1 s later than the one before, causing it to encounter a slightly different flow regime and plume structure. Second, a LW motion strategy which resembles Lévy-taxis in all but the turning angles which are drawn from a uniform distribution. Third, a CRW strategy, which resembles a Lévy-taxis in all but the move lengths which are taken from an asymptotically Gaussian ( $\mu = 3$ ) distribution. And fourth, a Brownian walk, in which move lengths are drawn from an asymptotically Gaussian-like ( $\mu = 3$ ) distribution, and turning angles are drawn from a uniform distribution. Effectively, in our simulations the LW is a special case of Lévy-taxis with  $\rho = 0$ , CRW is a special case of Lévy-taxis with  $\mu = 3$  and Brownian walk is a special case of Lévy-taxis with  $\rho = 0$  and  $\mu = 3$ .

Both CRW and LW are random walks that go beyond Brownian motion in the sense that they incorporate directional persistence in the walk. In CRW, directional persistence (i.e. the degree of directional or angular correlation in the random walk) is controlled by changing the shape parameter ( $0 \leq \rho \leq 1$ ) of the distribution of turning angles. When  $\rho = 0$ , turning angles exhibit a uniform distribution with no correlation between successive steps, resulting in Brownian motion. When  $\rho = 1$ , a delta distribution at  $0^\circ$  is achieved, leading to ballistic motion or straight-line walks. In LWs, the exponent of the power-law, the so-called Lévy index ( $1 < \mu \leq 3$ ), is the one controlling the range of correlations in the walk, so LW comprises a rich variety of paths ranging from Brownian motion ( $\mu \geq 3$ ) to straight-line paths [13] ( $\mu \rightarrow 1$ ). Both models have been widely used as models of animal movement at large scales [21–24].

## **Results**

Search strategies must compromise between spatial thoroughness and speed. Generally, those leading to high detection success rates (DS) are prone to low path directness (NGDR) and thus to low spatial and temporal efficiency. Conversely, strategies leading to a high NGDR do so at the price of low DS if searches are to be completed in a finite time. We quantitatively

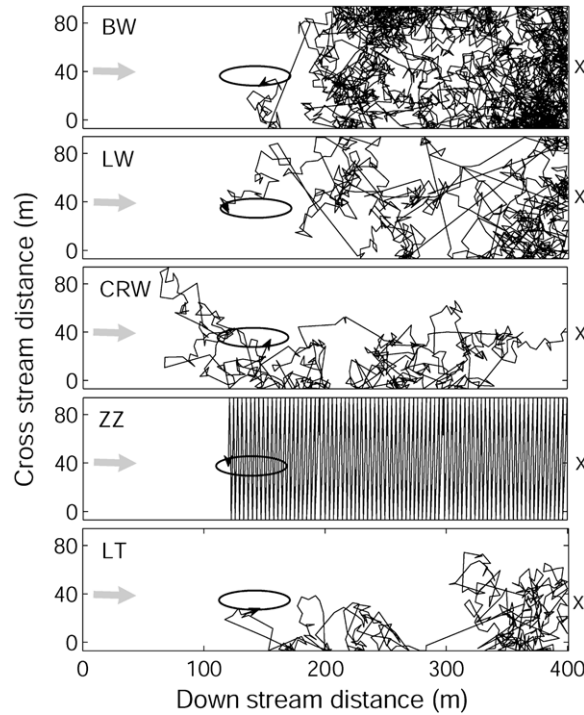


**Figure 2.** Characteristic trajectories of simulation runs. BW, Brownian walk ( $\mu = 3.0$ ,  $\rho = 0.0$ , DS = 70%, NGDR = 5.9%); CRW, correlated random walk ( $\mu = 3.0$ ,  $\rho = 0.05$ , DS = 77%, NGDR = 10.0%); LW, Lévy walk ( $\mu = 2.8$ ,  $\rho = 0.0$ , DS = 82%, NGDR = 6.4%); LT, Lévy-taxis ( $\mu = 2.8$ ,  $\rho = 0.05$ , DS = 82%, NGDR = 10.3%); ZZ, zig-zag (TA =  $89^\circ$ , DS = 100%, NGDR = 1.9%). Gray arrows are the mean direction of ambient flow. Trajectories begin at the X sign and end at the arrow sign. Runs end when the searcher arrives at the upstream boundary ('failure') or when odor is found ('success', i.e. concentration rises above noise threshold). In our simulations, noise level was 0.28% of the odor concentration at the plume's source. Odor sampling is continuous, i.e. occurs frequently within each 'step'. Ovals represent the location and size of the odor plume, although not its shape, since time averaging the plume creates a triangular shape. Due to plume intermittency, there are always areas within the plume where the chemical concentration falls below the detection threshold, so entering the oval does not ensure plume detection by the searcher.

characterized this tradeoff for five search strategies: BW (Brownian walk), LW (Lévy walk), CRW (correlated random walk), ZZ (zig-zag) and Lévy-taxis (figure 2). A critical feature in all search processes is the amount of directional persistence produced during the walk [13, 25]. In LW, CRW and ZZ, the directional persistence of the motion is controlled by the Lévy index  $\mu$  of the move length distribution ( $1 < \mu \leq 3$ ), the shape parameter  $\rho$  of the turning angle distribution ( $0 \leq \rho \leq 1$ ), and a fixed turning angle (TA) within the interval  $0^\circ \leq \text{TA} \leq 90^\circ$ , respectively. In our simulations, each of these three search strategies comprised a large variety of paths (figure 3): when the directional persistence decreased (i.e.  $\mu \rightarrow 3$  in LW,  $\rho \rightarrow 0$  in CRW and  $\text{TA} \rightarrow 90^\circ$  in ZZ), DS increased but at the price of a decreasing NGDR. At the lowest directional persistence for LW ( $\mu = 3$ ), CRW ( $\rho = 0$ ) and ZZ (TA =  $90^\circ$ ), the search resulted in a Brownian motion for the former two- and a one-dimensional casting motion for the latter. On the other hand, as the directional persistence increased in LW ( $\mu \rightarrow 1$ ), CRW ( $\rho \rightarrow 1$ ) and ZZ (TA  $\rightarrow 0^\circ$ ), NGDR increased but at the



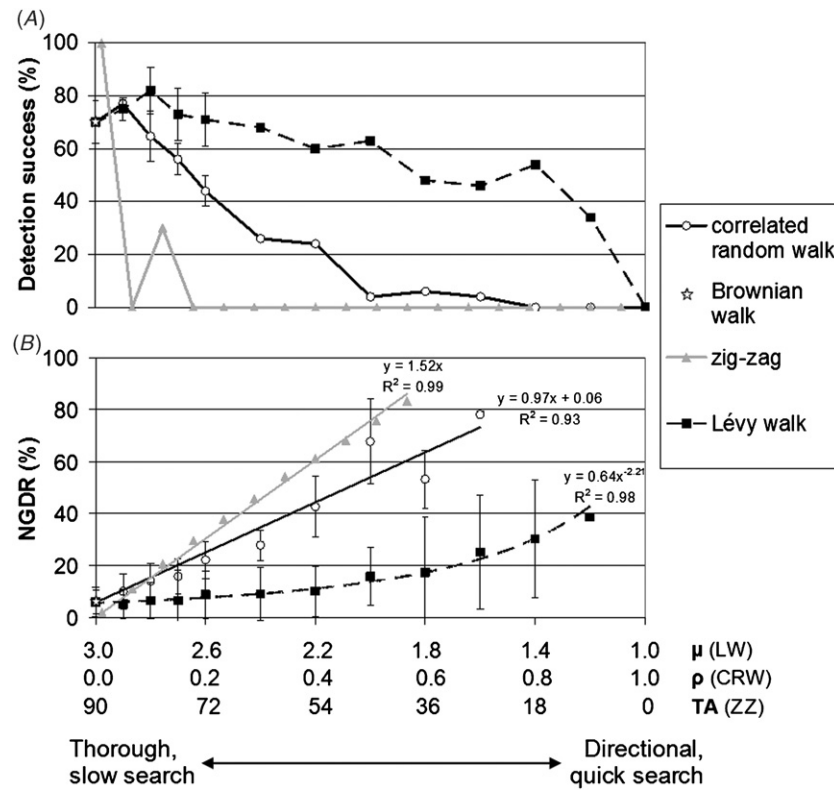


**Figure 3.** Plume-detection success (A) and NGDR (B, mean  $\pm$  SD) of simulations ( $N = 50$ ). Correlated random walks (CRW, white circles), Brownian walks (BW, white star), zig-zag (ZZ, gray triangles) and Lévy walks (LW, black squares). Lines in (B) are best-fits of the equations resulting in the highest  $R^2$  value possible. For both graphs,  $\mu$ ,  $\rho$  and TA serve as the x-axis for LW, CRW and ZZ, respectively. BW is at ( $\mu = 3$ ,  $\rho = 0$ ).

price of decreasing DS. At the highest directional persistence for LW ( $\mu = 1$ ), CRW ( $\rho = 1$ ) and ZZ (TA =  $0^\circ$ ), all the strategies resulted in straight-line trajectories (i.e. ballistic motion). Lévy-taxis, being a search strategy that combines both CRW and LW into a single strategy, exhibited in our simulations results similar to those of both LW and CRW: as the directional persistence decreased (i.e.  $\rho \rightarrow 0$ , and  $\mu \rightarrow 3$ ), DS increased while NGDR decreased (figure 4).

For each of the five search strategies, we ascertained the parameter ( $\mu/\rho/TA$ ) values that achieved the best DS, and the NGDR associated with those values. The best results for LW and CRW were achieved at  $\mu = 2.8$  and  $\rho = 0.05$  respectively, so it may come as no surprise that Lévy-taxis detection success peaked at ( $\mu = 2.8$ ,  $\rho = 0.05$ ). When plotting the settings of maximal plume-detection success against their respective NGDR values (figure 5), Lévy-taxis apparently combines the high DS of Lévy walks with the high NGDR of correlated random walks. An ANOVA test showed that significant differences existed between the NGDR values of the five search strategies ( $F = 90.9$ ,  $df = 4$ ,  $P < 0.001$ ), with subsequent  $t$ -tests verifying that the NGDR of Lévy-taxis was significantly higher than that of all other strategies except CRW ( $P < 0.001$ ). A second ANOVA test showed that significant differences existed between the DS values of the five search strategies ( $F = 16.9$ ,  $df = 4$ ,  $P < 0.001$ ), with subsequent

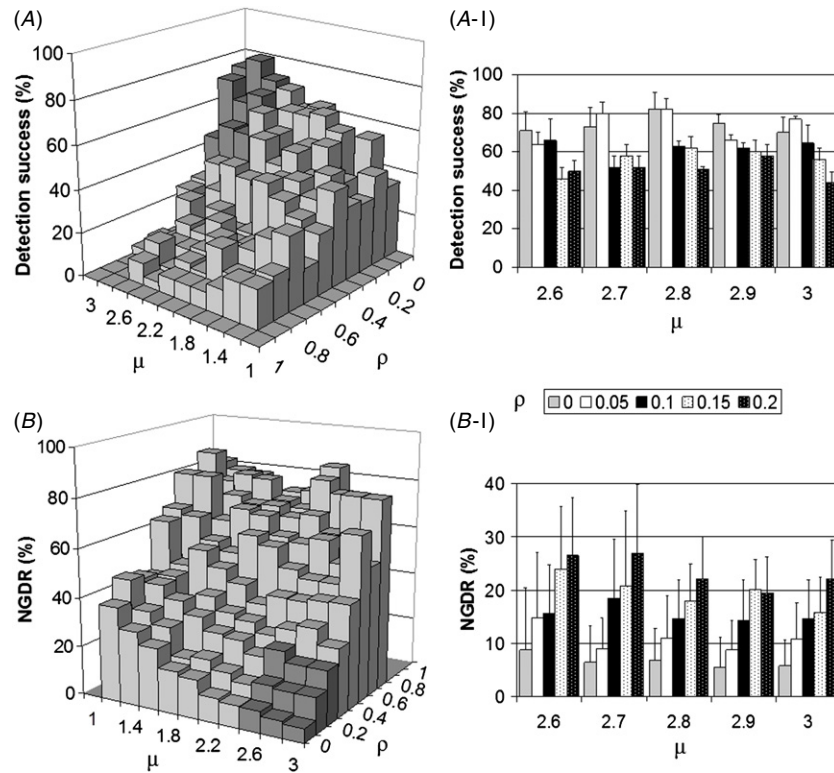


**Figure 4.** Plume-detection success (A) and NGDR (B) of the Lévy-taxis simulations ( $N = 50$  for each  $\mu/\rho$  combination). Note that the axes are inverted for clarity. The darker region ( $0 \leq \rho \leq 0.2$ ,  $2.6 \leq \mu \leq 3.0$ ) is detailed (mean  $\pm$  SD) in A-I and B-I, with color codes for  $\rho$  shown in the middle. Between  $1.0 \leq \mu \leq 2.6$ ,  $\mu$  was tested in increments of 0.2, with  $N = 50$  at each tested value; however, it was hypothesized that detection success would peak between  $2.6 \leq \mu \leq 3.0$ , so in this region  $\mu$  was tested in increments of 0.1 (to achieve a finer resolution), and the  $N = 50$  was repeated 5 times (to achieve a standard deviation value for the ‘detection success’ index). Similarly, Between  $0.2 \leq \rho \leq 1.0$ ,  $\mu$  was tested in increments of 0.1, with  $N = 50$  at each tested value; however, it was hypothesized that detection success would peak between  $0.0 \leq \rho \leq 0.2$ , so in this region  $\rho$  was tested in increments of 0.05 (to achieve a finer resolution), and  $N = 50$  was repeated 5 times (to achieve a standard deviation value for the ‘detection success’ index).

$t$ -tests attributing this difference to the DS of zig-zag which was significantly higher than all the others ( $P < 0.001$ ) as well as to the DS of Brownian walks which was significantly lower than all the others ( $P < 0.02$ ).

### Discussion

Under the particular conditions of our simulation, Lévy-taxis outperformed the rest of the stochastic search strategies, providing the best detection capability (matching that of LW) at the quickest speed (matching that of CRW). In the present study, the simulation environment, water flow and chemical plume were two dimensional. A main motivation for implementing the algorithms in 2D is the computational simplification achieved, but neutral buoyancy of the chemical or stratification of the flow [26] will often result in a plume of limited vertical

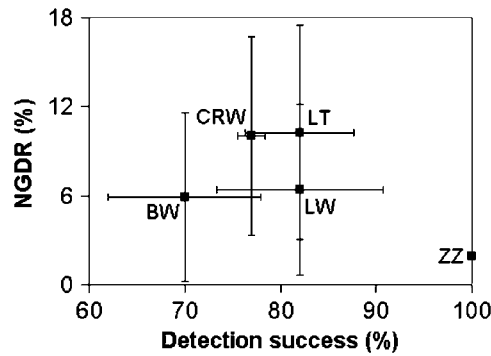


**Figure 5.** Plume-detection success and NGDR (mean  $\pm$  SD) for the parameter combination that achieved the best plume-detection success in each search strategy. BW, Brownian walk ( $\mu = 3.0$ ,  $\rho = 0.0$ ); CRW, correlated random walk ( $\mu = 3.0$ ,  $\rho = 0.05$ ); LW, Lévy walk ( $\mu = 2.8$ ,  $\rho = 0.0$ ); LT, Lévy-taxis ( $\mu = 2.8$ ,  $\rho = 0.05$ ); ZZ, zig-zag (TA =  $89^\circ$ ).

extent, which may be approximated as two dimensional. More important is the fact that we have considered only one flow regime and one realization of a plume, analyzing the effects of varying the walk path but not the flow/plume structure. It may be argued that in each of our simulation runs, the searcher experienced different flow/plume conditions because of the stochastic nature of its trajectory. In other words, within the confines of our single plume, each searcher experienced a different search process thanks to the inherent randomness of stochastic search strategies. Indeed, a key element of the model is the way the searcher gains information during its walk; this ‘information gain through time’ depends on both the walk itself and the plume structure. Nevertheless, it is clear that the ‘most efficient’ Lévy-taxis exponents found in this study are likely to change with the size of the system (the environment in which the search is taking place) and the size of the target (‘length’ and ‘width’ of the plume). For example, as the scale of the environment relative to the plume increases, one could expect the desired step lengths to increase, causing the ‘most efficient’ Lévy parameter to decrease until it reaches  $\mu \approx 2$  [27] in very large environments. Also, depending on the relative position of the searcher to the plume source, the long-term best strategy can be switched. For example, the Lévy-taxis tendency to move upstream means that, if the searching agent passes the plume source, it will tend, in subsequent steps, to move farther away from it. Thus, if the size of the plume is small relative to the environment, the LT strategy may actually prove less effective than a simple Lévy walk, which will be more likely to move back downstream (i.e. in the ‘correct’ direction). Because of all this, one should be careful not to draw too general conclusions from this specific experiment regarding the efficiency of Lévy-taxis. Instead, to get a more reliable picture of the robustness of the Lévy-taxis strategy it would be important to evaluate searching strategies by ensemble-averaging over many different plumes, because instantaneous plume structures in turbulent flows vary markedly between realizations. It is clear then that more experiments are needed, exploring the efficiency of the different search strategies at (i) different size scales of both environment and plume, (ii) different flow regimes and plume characteristics, and (iii) different starting points of the searching mission, e.g. upstream or cross-stream. It is important to emphasize that, in general, the solution to any search problem is highly sensitive to the specified initial and boundary conditions such as relative initial position of the searcher to the targets or the spatio-temporal scales. Nevertheless, clear physical pictures of the different instances in which a search solution is valid can be extracted if the underlying mechanisms are well understood [27].

Zig-zag strategies are common in insects (e.g. bees and moths [28]) and are adopted, for example, by male moths seeking plumes of female sex pheromone, but only after an odor filament has already been detected, i.e. only after the moth ‘knows’ that a nearby odor source is located upwind [29]. If a moth has no prior knowledge of odor source locations and if an odor cue has not been detected, then (depending on wind conditions) the moths move either in a crosswind or downwind direction [30]. If odor has not been detected then an odor source (if present) could be located far upwind (so that odor concentrations are diluted below the detection threshold); closer sources, on the other hand, could be located nearby in either the crosswind or downwind directions. Further studies are needed in order to adequately compare a more biomimetic zig-zag strategy (e.g. ‘odor-modulated anemotaxis’ [31]) to the other stochastic strategies, including Lévy-taxis; however, this was beyond the scope of the present study. In our work the zig-zag strategy merely attempted to serve as a control group representing a systematic (i.e. deterministic) search with an upstream component, given that all searchers started from a point downstream of the odor plume. As such, the plume-detection success of the best zig-zag setting was significantly higher than that of Lévy-taxis, but at the price of a very low NGDR. This effect is well known from other deterministic search strategies (e.g. Archimedean spiral [32]); such ‘slow thoroughness’ may be acceptable or even desirable when searching a very small area, but it is impractical for large-scale searches. Importantly, different plume/search area ratios may modify NGDR and DS, and thus, change the crossover of effectiveness between stochastic and deterministic strategies. In foraging animals, for example, behavioral shifts from deterministic to stochastic-like search strategies exist when the amount of time (or area) engaged on an unsuccessful deterministic search becomes large enough [13, 20].

The main novelty of Lévy-taxis navigation is in combining a Lévy walk with (a) a CRW-like orientation process and (b) environmental adaptiveness. As such, it differs from previous models that contain (a) but not (b) such as in Lévy-modulated CRWs [13], or (b) but not (a) such as in biased Lévy walks [30, 33]. Combining CRW and LW into a single motion strategy and using the flow intermittently as a dynamic guidance cue for navigation may prove of general importance in many aquatic and terrestrial search scenarios where there is an exploitable environmental signal that is spatially and coherently correlated to the target. In such cases, there is a bona fide, ubiquitous guidance cue that can lead the searching agent toward the true, much harder-to-find target. A good example for such search scenarios would be plume finding because the direction of the flow is directly correlated with the direction of the chemical plume [34]. Large-scale plume finding strategies might be universal in nature and of great applicability to real-world human missions. Our results show that incorporating adequate stochasticity that is compatible with relevant environmental information processing has the potential for significant advantages for real-world search strategies either by animals, humans or robotic agents. The Lévy-taxis navigation strategy has two major advantages for implementation in AVs (autonomous vehicles) engaged in plume-finding missions. First, its stochastic character accommodates the unpredictable nature of turbulence and the patchiness of odor plumes that it produces. Second, its guidance is derived entirely from local cues that are available on a short timescale with sole reliance on the ubiquitous and estimatable ambient flow. This is a distinct advantage over strategies that rely on remote guidance resources such as GPS systems; as such, Lévy-taxis may help AVs advance a step closer to true autonomy. Lévy-taxis, in addition to its merit in searching a large area for a chemical plume, may also be of use once the plume is found, efficiently following the plume to its source. This approach can potentially unify different phases of chemical source localization, e.g. plume-tracking and plume finding, as parametric variations of a single strategy instead of a series of ad hoc mechanisms. Furthermore, explorations of the biological plausibility of this proposition are

likely to prove fruitful in the field of ecology, explaining and predicting the movement patterns of various animals searching for food or mates.

### Acknowledgments

ZP was supported by an EC Marie Curie fellowship (MOIF-CT-2006-021733). FB has been supported by the Spanish Ministry of Science and Education (EX-2005-1011) and the National Science Foundation (DEB-0083566). We are grateful to Peter Santiago (Brooklyn College) and Kamil Kloskowski (Brooklyn College) for their dedication and insight, and to Pradeep Setlur (California State University, Sacramento) for assistance with programming. Todd Cowen (Cornell University) contributed the V3 data set, Jay Farrell (University of California, Riverside) shared the simulator source code, and Shaneen Singh (Brooklyn College) gave use of computing resources. Anibal de Almeida and Lino Marques (Coimbra University) provided comments on the work. Joseph Klafter (Tel-Aviv University) suggested the term ‘Lévy-taxis’ for our search strategy. We are also indebted to two anonymous reviewers for their important and thoughtful comments which greatly improved the manuscript.

*Funding.* Z Pasternak was supported by an EU FP6 Marie Curie OIF grant. F Bartumeus is pleased to acknowledge the support of the Spanish Ministry (EX-2005-1011), the National Science Foundation (EF-0434319), and DARPA (HR0011-05-1-0057). The funders had no role in study design, data collection and analysis, decision to publish or preparation of the manuscript.

### References

- [1] Viswanathan G M, Raposo E P and da Luz M G E 2008 Lévy flights and superdiffusion in the context of biological encounters and random searches *Phys. Life Rev.* **5** 133–50
- [2] Vickers N J 2000 Mechanisms of animal navigation in odor plumes *Biol. Bull.* **198** 203–12
- [3] Grasso F, Consi T R, Mountain D C and Atema J 1999 Biomimetic robot lobster performs chemo-orientation in turbulence using a pair of spatially separated sensors: progress and challenges *J. Robot. Auton. Syst.* **807** 1–17
- [4] Grasso F W and Atema J 2002 Integration of flow and chemical sensing for guidance of autonomous marine robots in turbulent flows *J. Environ. Fluid Mech.* **1** 95–114
- [5] Marques L, Nunes U and Almeida A T 2002 Olfaction-based mobile robot navigation *Thin Solid Films* **418** 51–8
- [6] Russell R A, Bab-Hadiashar A, Shepherd R L and Wallace G G 2003 A comparison of reactive robot chemotaxis algorithms *Robot. Auton. Syst.* **45** 83–97
- [7] Farrell J A, Pang S and Li W 2005 Chemical plume tracing via an autonomous underwater vehicle *IEEE J. Ocean Eng.* **30** 428–42
- [8] Pyk P *et al* 2006 An artificial moth: chemical source localization using a robot based neuronal model of moth optomotor anemotactic search *Auton. Robots* **20** 197–213
- [9] Vergassola M, Villermaux E and Sharaiman B I 2007 ‘Infotaxis’ as a strategy for searching without gradients *Nature* **445** 406–9
- [10] Liao Q and Cowen E A 2002 The information content of a scalar plume—a plume tracing perspective *J. Environ. Fluid Mech.* **2** 9–34
- [11] Weissburg M J *et al* 2002 A multidisciplinary study of spatial and temporal scales containing information in turbulent chemical plume tracking *J. Environ. Fluid Mech.* **3** 65–94
- [12] Bellingham J G, Goudey C A, Consi T R and Chryssostomidis C 1992 A small, long-range autonomous vehicle for deep ocean exploration *Proc. 2nd Int. Offshore Polar Eng. Conf.*
- [13] Bartumeus F, da Luz M G E, Viswanathan G M and Catalan J 2005 Animal search strategies: a quantitative random-walk analysis *Ecology* **86** 3078–87
- [14] Shlesinger M F and Klafter J 1986 Lévy walks versus Lévy flights *On Growth and Form* ed H E Stanley and N Ostrowski (Amsterdam, The Netherlands: Martinus Nijhof Publishers) pp 279–83
- [15] Kareiva P M and Shigesada N 1983 Analyzing insect movement as a correlated random walk *Oecologia* **56** 234–8

- [16] Vogel S 1996 *Life in Moving Fluids* (Princeton, NJ: Princeton University Press) p 484
- [17] Viswanathan G M *et al* 2000 Lévy flights in random searches *Physica A* **282** 1–12
- [18] Viswanathan G M *et al* 2001 Lévy flight search patterns of biological organisms *Physica A* **295** 85–8
- [19] Bovet P and Benhamou S 1988 Spatial analysis of animals' movements using a correlated random walk model *J. Theor. Biol.* **131** 419–33
- [20] Hoffman G 1983 The random elements in the systematic search behaviour of the desert isopod *Hemilepistus reaumuri* *Behav. Ecol. Sociobiol.* **13** 81–92
- [21] Turchin P 1998 *Quantitative Analysis of Movement* (Sunderland, MA: Sinauer)
- [22] Bergman C M, Schaefer J A and Luttich S N 2000 Caribou movement as a correlated random walk *Oecologia* **123** 364–74
- [23] Bartumeus F, Peters F, Pueyo S, Marrase C and Catalan J 2003 Helical Lévy walks: adjusting searching statistics to resource availability in microzooplankton *Proc. Natl. Acad. Sci. USA* **100** 12771–5
- [24] Bailey H and Thompson P 2006 Quantitative analysis of bottlenose dolphin movement patterns and their relationship with foraging *J. Anim. Ecol.* **75** 456–65
- [25] Bartumeus F, Catalan J, Viswanathan G M, Raposo E P and da Luz M G E 2008 The influence of turning angles on the success of non-oriented animal searches *J. Theor. Biol.* **252** 43–55
- [26] Stacey M T *et al* 2000 Plume dispersion in a stratified, near-coastal flow: measurements and modeling *Cont. Shelf Res.* **20** 637–63
- [27] Bartumeus F and Catalan J 2009 Optimal search behavior and foraging theory *J. Phys. A: Math. Theor.* **42** 434002
- [28] Dusenbery D B 1990 Upwind searching for an odor plume is sometimes optimal *J. Chem. Ecol.* **16** 1971–6
- [29] Sabelis M W and Schippers P 1984 Variable wind directions and anemotactic strategies of searching for an odour plume *Oecologia* **63** 225–8
- [30] Reynolds A M, Reynolds D R, Smith A D, Svensson G P and Löfstedt C 2007 Appetitive flight patterns of male *Agrotis segetum* moths over landscape scales *J. Theor. Biol.* **245** 141–9
- [31] Balkovsky E and Shraiman B I 2002 Olfactory search at high Reynolds number *PNAS* **99** 12589–93
- [32] Zollner P A and Lima S L 1999 Search strategies for landscape-level interpatch movements *Ecology* **80** 1019–30
- [33] Reynolds A M 2005 Scale-free movement patterns arising from olfactory-driven foraging *Phys. Rev. E* **72** 041298
- [34] Viswanathan G M *et al* 1999 Optimizing the success of random searches *Nature* **401** 911–4